Sensors & Actuators: B. Chemical 320 (2020) 128381

Contents lists available at ScienceDirect

Sensors and Actuators B: Chemical

journal homepage: www.elsevier.com/locate/snb

Electrochemical Dissolved Oxygen Sensor-Integrated Platform for Wireless In Situ Bioprocess Monitoring

Justin M. Stine[a,b], Luke A. Beardslee[b], Rajendra M. Sathyam[a], William E. Bentley[c,d,e], Reza Ghodssi[a,b,d,e,*]

[a] Department of Electrical & Computer Engineering, University of Maryland, College Park, MD, 20742, USA
[b] Institute for Systems Research, University of Maryland, College Park, MD, 20742, USA
[c] Institute for Bioscience & Biotechnology Research, University of Maryland, College Park, MD, 20742, USA
[d] Robert E. Fischell Institute for Biomedical Devices, University of Maryland, College Park, MD, 20742, USA
[e] Fischell Department of Bioengineering, University of Maryland, College Park, MD, 20742, USA

ARTICLE INFO

Keywords:
Dissolved Oxygen
Bioreactor
Bluetooth Low Energy
Clark-type Sensor
Wireless Electronics

ABSTRACT

This work presents a bio-processing online device (bPod) platform, capable of real-time *in situ* monitoring of bioreactor cell culture parameters, such as dissolved oxygen (DO). The bPod is an integrated system comprised of a potentiostat analog-front-end (AFE), a Bluetooth Low Energy (BLE) microcontroller, and a chemical sensor, exemplified here by a Clark-type DO sensor, which enables monitoring of dissolved oxygen content. The Clark-type electrochemical sensor performs chronoamperometric measurement of DO percent saturation, and the BLE microcontroller wirelessly transmits data to a smartphone while submerged in aqueous media. After several electrode design modifications, the bPod showed a linear electrochemical current response corresponding to DO percent saturation levels with a sensitivity of 37.5 nA/DO% and limit of detection of 8.26 DO%, covering concentration ranges relevant for mammalian culture processes within bioreactors. The wireless bPod provides a free-floating capsule architecture for monitoring DO and can be adapted for an array of electrochemical sensors, targeting different process parameters for diverse bioprocess monitoring applications.

1. Introduction

Recent advancements in continuous bioprocess monitoring have enabled rapid, high quality, and high throughput production of a wide variety of mammalian and bacterial cell cultures for pharmaceutical products (i.e., biopharmaceuticals, antibiotics, and vaccines). By far, monoclonal antibodies (mAbs) are the dominant biotherapeutic on the market; they are also among the most important reagents in biologically related research [1–3]. Monoclonal antibodies are produced in large fully automated bioreactors and are synthesized by recombinant cell lines (primarily of the Chinese hamster ovary, CHO) cultivated in carefully designed cell culture media [4].

Existing commercial monitoring technologies, such as inline instrumental probes, represent a single-point measurement, taken as the averaged value for an entire cell reactor. A major concern is their inability to detect the presence of gradients or heterogeneity in physical parameters (i.e. temperature/pH) and the concentration of compounds of interest (i.e. glucose/oxygen) throughout the bioreactor [5,6]. More specifically, varied distributions of common process parameters such as dissolved oxygen (DO), pH, dissolved CO_2 (dCO_2), and glucose, are known to be a significant source of non-uniformity for mammalian cells and related proteins in large-scale bioreactors [7]. In addition, formation of either hypoxic or hyperoxic regions produce varied glycosylation patterns [8,9], charge variants [10], aggregates [11], and low-molecular-weight species [12], causing inconsistent performance of the manufactured byproducts. Understanding the impact of heterogeneities in process parameters on cell culture quality is critical for obtaining higher process yields and more effective molecular products. Therefore, sensors that can permeate the bioreactor flows and record spatially relevant information are in high demand to achieve high precision bioprocess monitoring.

Among the culture parameters of interest, DO plays a critical role in cell proliferation in batch cultures and various bioreactor systems that maintain a homogeneous oxygen distribution to achieve high cell densities. As biomass increases, so too does the demand for DO, where poor distribution of DO can form hypoxic zones which can result in micro-heterogeneities of the culture products, resulting in production of biologics with heterogeneous attributes. In most bioreactor systems,

* Corresponding author at: Department of Electrical & Computer Engineering, Kim Building 2236, University of Maryland, College Park, MD, 20742, USA.
E-mail address: ghodssi@isr.umd.edu (R. Ghodssi).

https://doi.org/10.1016/j.snb.2020.128381
Received 5 March 2020; Received in revised form 27 May 2020; Accepted 28 May 2020
Available online 30 May 2020
0925-4005/

standard DO measurements typically rely on oxygen transport through a gas permeable membrane [13]. In general, optical sensors are resilient to flow and have greater sensitivity at lower DO concentrations, compared to electrochemical sensors [14]. However, inline optical sensors often have slower response times (~30 s) and higher energy consumption than their electrochemical counterparts (~9 s). This tends to hinder low-powered monitoring approaches that dynamically sample within a bioreactor.

To this end, amperometric electrochemical sensors are most suitable for interrogation of localized DO distributions in bioreactors. The Clark-type sensor topology has been extensively explored for DO and exhibits excellent linearity across a variety of biomedical and biomanufacturing applications [15–18]. Most cell culture bioreactors utilize varied flows of compressed gases and stirring speeds in order to control for the DO at specific set points usually between 20–50% of air saturation [19,20]. On-line and automated measurements are essential to correct dissolved oxygen drift and promote homogeneity [21]. Most notably, integration of sensors with wireless monitoring systems have shown potential to allow for significant improvements in process scale up and bioreactor optimization [22]. Radio frequency identification (RFID) tags capable of passively interrogating the reactor headspace have been demonstrated for monitoring temperature and pressure within single-use bioreactors [23–25]. The RFID tags are affixed to the bioreactor walls, wirelessly powered using an external source, and directly sterilized. However, RFID tags utilize near-field communication standards, which limits their use to glass and plastic walled vessels and requires scaling of the antenna size with increasing bioreactor volumes. They also are limited to headspace and are not typically used to monitor media analytes.

There have been only a few reports demonstrating free-floating wireless sensors capable of liquid measurements and that do not require a physical connection to the bioreactor [26–29]. Todtenburg et al. developed a capsule for detecting biochemical parameters, such as pH, glucose, and conductivity within a photobioreactor. By integrating CMOS circuitry and COTS components, the device wirelessly transferred pH and RSSI data to an external receiver. The capsule consists of a waterproof top to protect the electronics and a liquid permeable bottom to expose the sensor to the culture media [27]. Zimmerman et al. have utilized sensor spheres to characterize fluid dynamics within turbulent flows of an aerated bioreactor [28]. The sensors modules were reported to be neutrally buoyant monitoring capsules fabricated from poly ether ketone (PEEK), known as smartCAP (smartINST, Lyon, France), which support several sensing modalities, including temperature, conductivity, and agitation [30]. Among the examples provided above, an *in situ* wireless monitor of DO using free-floating sensors in bioreactors has not yet been achieved.

Similar microsystems have also been developed for vastly different biologic environments, such as ingestible electronics or human wearables. For example, Caffrey et al. developed an ingestible capsule system capable of monitoring temperature, pH, and DO in the human gastrointestinal tract (GI). This microsystem was later redesigned for use in single-use bioreactors, where the capsule was allowed to freely move around the bulk media of the bioreactor, however, transitioning sensing capabilities from the human GI tract environment to the bioreactor has yet to be realized [5,31]. Additionally, commercial approaches for integrating microfabricated sensors with telecommunication have been developed, such as a blood glucose monitoring system created by FreeStyle Libre, which similarly performs real-time continuous measurement [32]. By these examples, we and others are motivated to integrate commercial-off-the-shelf (COTS) components with wireless modules for targeting specific environments [33–38]; however, the implementation of free floating systems specifically in bioreactors, have yet to be fully addressed, and extracting relevant cell culture information using integrated *in situ* sensors, telecommunication capabilities, and biocompatible packaging remains a challenge.

In this work, a fully integrated free-floating platform was developed for real-time, wireless, and *in situ* electrochemical monitoring of chemical analytes. While we envision measurements of glucose, glutamine, and lactate, we have first explored DO, owing to its importance in maintaining cell productivity. The device is housed within a leak-proof 3D-printed package and utilizes a potentiostat analog-front-end (AFE) paired with a BLE system-in-package (SiP) microcontroller for data processing and wireless data transmission. The AFE is connected to an amperometric electrochemical DO sensor, utilizing microfabrication techniques to achieve a miniaturized Clark-type sensor topology. Electrochemical characterization resulted in an optimal voltage bias, determined through cyclic voltammetry, allowing real-time chronoamperometric detection of different DO percentages (DO%) using the bPod under dynamically changing sparging conditions in DI water. The current system is comprised of off-the-shelf electrical components, a carefully designed and assembled Clark-type oxygen sensor, and a 3D-printed housing for leak proof operation. The current bPod is 60 mm in diameter and is deployed here as a prototype that will be scaled down to less than half the current size for use in lab and pilot scale reactors. Overall, this work highlights the integration and design of key system components that specifically address challenges associated with wireless sensing within bioreactors yielding a proof-of-concept system for DO monitoring.

2. Materials and methods

2.1. Chemicals

Potassium chloride (KCl), used for preparing 0.1 M electrolyte solution, was obtained from Sigma Aldrich (St. Louis, MO) and used without further purification. Sparging conditions in the bioreactor were generated using compressed nitrogen (N_2) and oxygen (O_2) gas cylinders (K-type), purchased from Airgas (Radnor Township, PA). De-ionized (DI) water (> 18 MΩ-cm) was obtained from an E-pure Ultrapure Water Purification Systems (Thermo Scientific, Waltham, MA).

2.2. bPod system overview

An overview of the system operation is shown in Fig. 1. The bPod

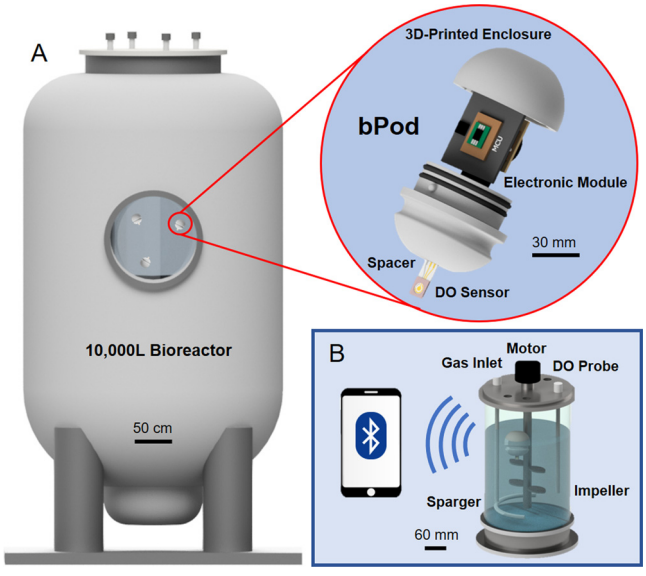

Fig. 1. (A) Overview schematic detailing implementation of the wireless bPod platform within an industrial-scale bioreactor. System components include an electronic module, electrochemical DO sensor, and 3D-printed enclosure. (B) The platform is evaluated in a bench-scale bioreactor (10-L) and data is obtained using Bluetooth Low Energy communication between the bPod and a mobile phone.

platform was designed for implementation into large-scale bioreactors and contains three main components: the electronic module, a leak-proof 3D-printed package, and the electrochemical DO sensor. The electronic module utilizes a BLE chipset and a portable potentiostat AFE to enable amperometric monitoring of DO. The microcontroller is programmed to remain in a low-power mode, only waking up periodically to perform measurements and wirelessly transmit data to a modified phone app. The leak-proof packaging is 3D-printed using biocompatible MED610 to isolate the electronics from the liquid environment. The electrochemical DO sensor is fabricated using a three-electrode amperometric configuration for chronoamperometry, allowing quantification of oxygen partial pressure [39]. To establish an electrolyte reservoir for the sensor, a fluorinated ethylene propylene (FEP) membrane is attached to the sensor surface, encapsulating potassium chloride (0.1 M KCl) electrolyte onto the electrodes, creating an oxygen selective barrier between the bioreactor solution and the KCl electrolyte to enable measurement of DO partial pressure. The platform is evaluated at the bench scale in a 10-L BioFlo 310 fermenter with data recorded wirelessly to a phone using BLE (Fig. 1B).

2.2.1. Fabrication and assembly of Clark-type dissolved oxygen sensor

Here, a three-electrode sensor with a thin-film gold (Au) working electrode (4 mm diameter), gold counter electrode, and a silver (Ag) reference electrode is fabricated as depicted in Fig. 2A. Cr/Au (20 nm/200 nm) layers were deposited onto a 4-inch Pyrex wafer using an Angstrom E-beam Evaporator (Angstrom Engineering Inc.), followed by deposition of Ag (250 nm) for the reference electrode. The concentric electrodes are patterned via use of a laser cut (Epilog Laser Fusion M2 laser cutter) shadow mask made of cleanroom paper, which was affixed to the Pyrex wafer. The mask was first taped to the edges of the wafer surface for the working and counter electrodes, which were subsequently covered for deposition of the silver reference electrode. The wafer is then diced into individual sensors (9 mm × 20 mm) using a dicing saw (Microautomation) and cleaned with a combination of acetone, methanol, and isopropanol, followed by rinsing with DI water and drying with nitrogen gas.

An electrolyte solution reservoir is created above the Clark-type electrode, using electroplating tape (118 µm) (3 M Type-470, Maplewood, MN) and a FEP membrane (25 µm) (Strathkelvin, North Lanarkshire, Scotland). Electroplating tape had shown to be both moisture and chemically resistant, as well as capable of forming a watertight interface between the Pyrex surface. Two layers of electroplating tape are aligned with the sensor contacts and cut to form a 5 mm circular well using a biopsy punch. The first tape layer is adhered directly to the glass substrate centered around the concentric sensor, and 20 µL of electrolyte solution (0.1 M KCl) is pipetted onto the electrode surface. The circular tape opening prevents the electrolyte solution from spreading and shorting the contact pads. Using the second tape layer, a small FEP membrane square (7 mm × 7 mm) is brought into contact with the KCl droplet and carefully sealed by applying pressure between the first and second tape layers, such that no bubbles are trapped in the reservoir. A summary of the assembly process is provided in Supplemental Fig. 1. This method of encapsulation is compatible with low electrolyte volumes (20 µL) and reduces the distance between the FEP membrane and the sensor surface (on the order of the FEP membrane thickness), ensuring that only diffusion through the FEP membrane would limit sensor response time (T. J. Kim et al., 2001). The KCl electrolyte, provides ions that enhance electron transport, allowing the reduction of oxygen at the working electrode surface, as illustrated in the sensor cross-section of Fig. 2A [40]. To prevent evaporation of the electrolyte solution through the FEP membrane, the sensors were stored in DI water between successive trials. Park et al. have achieved a similar DO sensor using a 3-electrode configuration with Au working and Ag/AgCl reference electrode on a glass substrate.

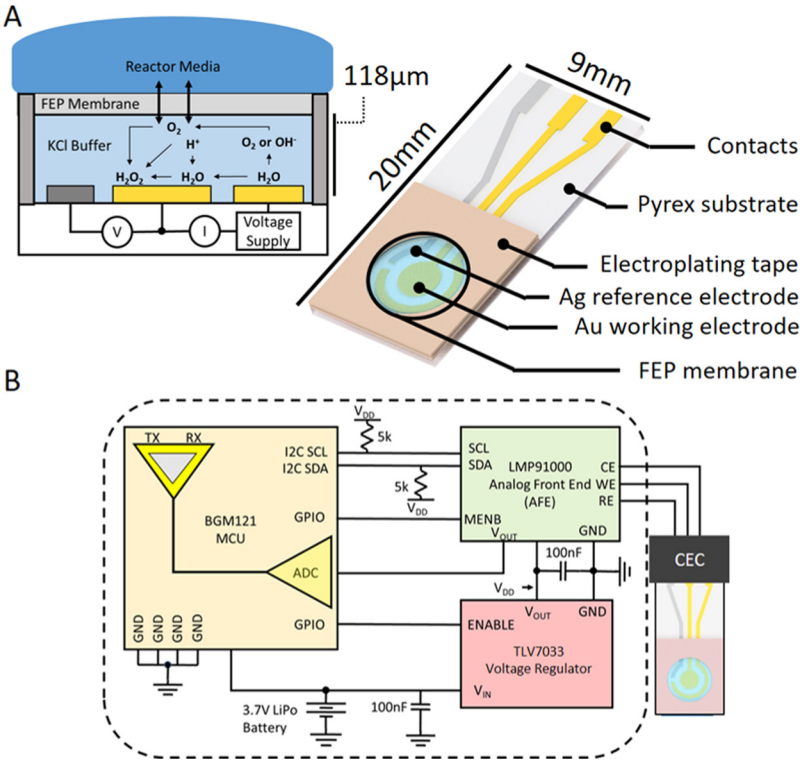

Fig. 2. System components. (A) Illustration of assembled DO sensor and a cross-sectional diagram of the chemical reaction for the Clark-type electrode. The electrolyte solution is injected at very low volume (20 μ L) and the distance between the reactor and the electrode is 118 μ m (for rapid diffusion).The oxygen reduction reaction is measured using a three-electrode system with gold working and counter electrodes, and a silver reference electrode. (B) Circuit schematic of the electronic module, including the BGM121 microcontroller and LMP91000 readout circuit. Chronoamperometric measurements are performed by the AFE and controlled by the BLE MCU to allow for portable and wireless monitoring of DO.

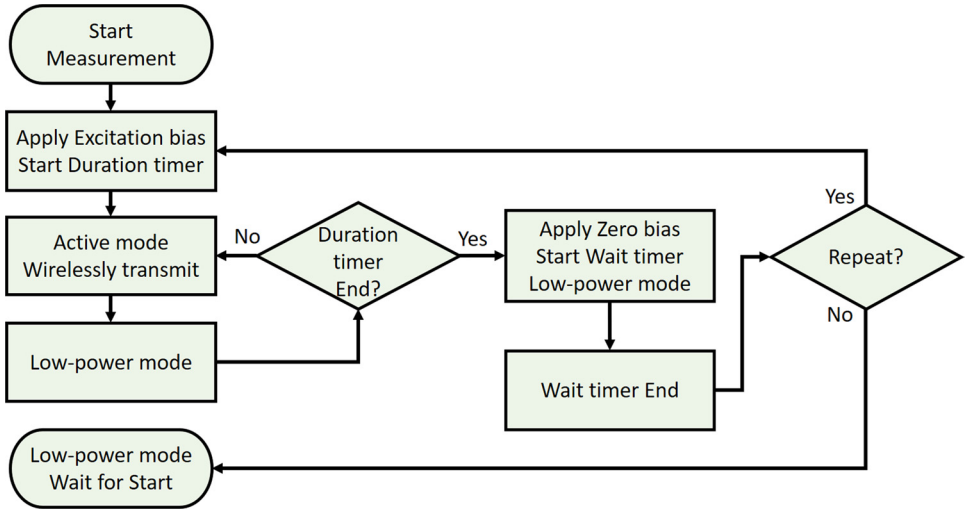

Fig. 3. Process flow for measurement sequence.

They used a fluorinated ethylene propylene (FEP) membrane and trapped an electrolyte using a molded PDMS structure to achieve rapid sensor response [15]. While this assembly strategy allowed for minimal distance between the sensor surface and FEP membrane, the permeability of the PDMS was not ideal for long-term DO monitoring as compared to our tape-based sensor approach.

2.2.2. System enclosure

bPod biocompatibility and electronics preservation is achieved by packaging the sensor and electronic module in a 3D-printed MED610 enclosure, printed using a Connex Objet500 PolyJet printer (Stratasys, Eden Prairie, MN). MED610 is biocompatible, autoclavable, and exhibits low liquid retention. The spherical pod, with an outer diameter of 60 mm, is assembled from two attachable parts as shown in Fig. 1A. The two halves (top and bottom) of the packaging are connected via a bayonet twist lock and sealed with three silicone O-rings. A small rectangular slit (10 mm × 2 mm) is used to align the DO sensor with a card edge connector (CEC) for interfacing with the electronic module. To provide a robust connection between the sensor contacts and the CEC, a tapered spacer was utilized to add thickness to the sensor and to provide support during system testing and sensor replacement. To prevent leaking between the DO sensor and the 3D-printed enclosure, the rectangular slit was sealed with epoxy. Following a trial with the assembled bPod, the DO sensor was replaced by removing the epoxy seal and inserting another DO sensor.

2.2.3. Design of wireless amperometric circuit

A simplified schematic of the electronic module is shown in Fig. 2B. A BLE 4.0 microcontroller was chosen for data processing and transmission to an external user device, such as a mobile phone or laptop. Specifically, the BGM121 SiP chipset used (6.5 mm × 6.5 mm × 1 mm) includes a programmable microcontroller and an integrated 2.45 GHz transceiver antenna (0 to +8 dBm). The BGM121 utilizes several energy saving modes to control current consumption depending on the required function, thus, extending the operational lifetime of the device. When transmitting and receiving data, the device enters 'active mode' and draws 25 mA of current. While idling for an event interrupt to occur, the device is set in 'low-power' mode, consuming 2.5 µA. Additionally, to further minimize power consumption, a temporary shutdown of the device is available using 'hibernate' mode, which consumes 0.58 µA. The available peripherals include a 12-bit analog-to-digital converter (ADC), several GPIO pins used for toggling the enable pin of the AFE, and two I^2C lines allowing bidirectional communication between the amperometric circuit and MCU. An LMP91000 AFE potentiostat was chosen to provide a stable voltage bias, or excitation voltage, between the working and reference electrodes of the sensor and monitor the resulting output current. The currents measured at the working electrode are converted into a voltage by a transimpedance amplifier, then digitized by the BGM121 ADC. The LMP91000 was programmed using an I^2C interface to toggle between an internal sleep mode and a three-electrode amperometric configuration. The electronic module is powered by a single 3.7 V lithium polymer (Li-Po) battery (GM301014H, PowerStream) with 14 mA h capacity. A 3.3 V linear voltage regulator (TLV7033, Texas Instruments) was used to stabilize and step-down the battery output for each of the electronic components. Finally, the electronic module is attached to a 3-pin CEC (2.54 mm pitch) to interface with the DO sensor assembly.

2.2.4. Event scheduling for wireless transmission

The BGM121 microcontroller was programmed to receive commands from a modified BLE smartphone app (Silicon Labs) for data acquisition and setting the device into one of three operational states: OFF, MEASURE, and CALIBRATE. The default energy mode of the device is 'low-power' mode. The oxygen level in the reactor equilibrates rapidly with the electrolyte; this in turn is measured using chronoamperometry, where an excitation voltage is applied over a short time window across the working and reference electrodes and read as current. Current values are recorded and transmitted every 50 ms for 30 s to produce a characteristic chronoamperometric response; this is defined as the measurement sequence. The CALIBRATE state performs a single measurement sequence used to perform single-point measurements desired for calibrating the bPod at both air-saturated and nitrogen-saturated conditions. Similarly, the MEASURE state will repeat the measurement sequence a user-defined number of times at a 5 min interval. Between measurements, the working and reference electrodes are shorted to ground by the LMP91000, and the bPod is maintained in 'low-power' mode, as described in section 2.2.3. Once the desired amount of data has been collected, the device will return to 'low-power' mode until another external command is given. The process flow for the MEASURE operational state is shown in Fig. 3; the measurement duration is defined as the Duration timer, and the measurement interval is defined as the Wait timer. The OFF state enters the device into the 'hibernate' mode, effectively turning off the MCU so that it consumes minimal current. In this mode, the device disconnects from the phone app and enables assembly of the bPod and sensor replacement between experiments. Using the software timers and external write commands available for BLE communication allows the state of the bPod to be user-controllable in real time and enables the bPod to operate autonomously when electrochemically monitoring DO percent saturation.

2.3. Electrochemical characterization and calibration

Electrochemical characterization of the bPod was performed in three separate settings: (1) a 250 mL beaker for the DO sensor assembly, using a benchtop potentiostat, (2) a 2 L vessel for optimizing bPod testing parameters, and (3) a 10-L BioFlo 310 bioreactor for dynamically monitoring the bPod platform at several DO saturation percentages.

2.3.1. Beaker-level DO sensor characterization

Beaker-level testing utilized cyclic voltammetry and chronoamperometry, performed by a VSP-300 BioLogic potentiostat (Warminster, PA) to determine an excitation voltage and evaluate the dynamic current range of the fabricated DO sensor. The electrochemical analysis of the three-electrode system was first conducted in 0.1 M KCl at room temperature. 0% and 100% DO saturation states were created by flowing N_2 and compressed air into the solution for 10 minutes, respectively. Separate gas lines were connected to a 250 mL beaker using polyethylene tubing and filtered through a stone bubble diffuser to improve solubility of the DO in the solution. Since the FEP membrane was not attached during the beaker-level testing, sparging of N_2 and compressed air into the beaker was interrupted during electrochemical evaluation in order to avoid interference of the measured signal due to bubbles. Cyclic voltammetry was performed by sweeping a linear voltage from -0.1 to -0.6 V at a scan rate of 20 mV/s. To evaluate the ion impermeability of the FEP membrane and the efficacy of the tape-based sensor interface, DO sensors with and without the FEP membrane attached were compared (see section 2.2.1) in an ambient DO% saturation (~20 %) in DI water. Cyclic voltammetry was performed by sweeping a linear voltage from 0 to -0.65 V at a scan rate of 20 mV/s. This verification step was repeated for each assembled DO sensor prior to integration with the bPod. To account for discrepancies in the testing system and sensor fabrication, a two-point calibration of the DO sensor and bPod was performed in the 2 L glass vessel, as shown in Supplemental Fig. 2. DO% was calculated based on the current response in an air-saturated state and a N_2-saturated state using the determined excitation voltage. A saturation state was produced by sparging 0.1 M KCl with either air or N_2 at room temperature for 10 minutes and using a polarographic DO electrode to ensure steady state. Testing parameters, including measurement duration, sampling rate, and transimpedance amplifier (TIA) gain, were adjusted for evaluation in the 10-L bioreactor and are described in the Supplementary information.

2.3.2. Electrochemical evaluation of bPod in 10-L bioreactor

After testing the performance of the DO sensor in 0.1 M KCl and DI water, the electronic module was integrated with the DO sensor in the bPod enclosure, as described in section 2.2.2. The bPod was placed into the 10-L bioreactor setup, as shown in Fig. 1B, filled with DI water, and tethered to minimize measurement failures from collisions, as well as connected to an external 3.3 V power supply (Agilent, Santa Clara, CA). In order to generate the various DO saturation states, two pressure regulated (5 psi) inputs of O_2 and N_2, respectively, were inserted into the BioFlo 310 fermenter and combined using a built-in flow controller. A single gas inlet was then connected to the 10-L vessel with polyethylene tubing, and gases were bubbled into the solution at a set volumetric flow rate (2.0 SLPM) and varied by adjusting the percent ratio of O_2 and N_2 (O_2:N_2). For each configuration, saturation points were determined after 15 minutes of sparging and referenced to a commercial polarographic DO probe (Mettler Toledo, Columbus, OH). The solution was stirred using an impeller speed of 75 rpm throughout all experiments, coinciding with lower rpm used for mammalian cell culture [41]. Chronoamperometric measurements of DO were performed under the chosen excitation voltage using the CALIBRATE command described in section 2.2.4. The oxygen level in the bioreactor's aqueous media is typically normalized as a percentage of the total saturated DO concentration. The level varies greatly depending on the cell density, pressure, tank agitation, flow rate of the gas mixtures, and temperature. Prior to assessing intermediate oxygen concentrations, the bPod sensor was calibrated at room temperature in DI water using two set points, a nitrogen-saturated state (0:100) and oxygen-saturated state (100:0), which equates to an oxygen concentration of ~8.9 mg/L. Following 15 minutes of sparging under each configuration, the measured DO sensor voltage output was assigned to 0 and 100% DO saturation states, respectively. The current response of the sensor corresponds to positive readout voltage from the bPod (between 0 and 1.65 V), calculated as shown in Supplemental Eq. (1). Increasingly negative currents correspond to values closer to 0 V and are dependent on the previously set current bounds. The sensitivity and limit of detection of the DO sensor are determined from a calibration plot and expressed in terms of the sensor current output.

2.3.3. Validation of fully integrated bPod

For real-time monitoring, the 3.7 V Li-Po battery was connected to the electronic module, and the bPod was left untethered and suspended within the 10-L bioreactor filled. The MEASURE command was used to record a measurement every 5 minutes for 1.5 hours (18 total), while the DO% saturation was varied incrementally between 0 and 100% every 10 minutes and compared to a commercial inline DO probe. Data was wirelessly transmitted by the BGM121, which was powered by the 3.7 V Li-Po battery. By utilizing external commands and the low-power energy modes of the BGM121, the bPod lifetime was estimated to be roughly 30 hours.

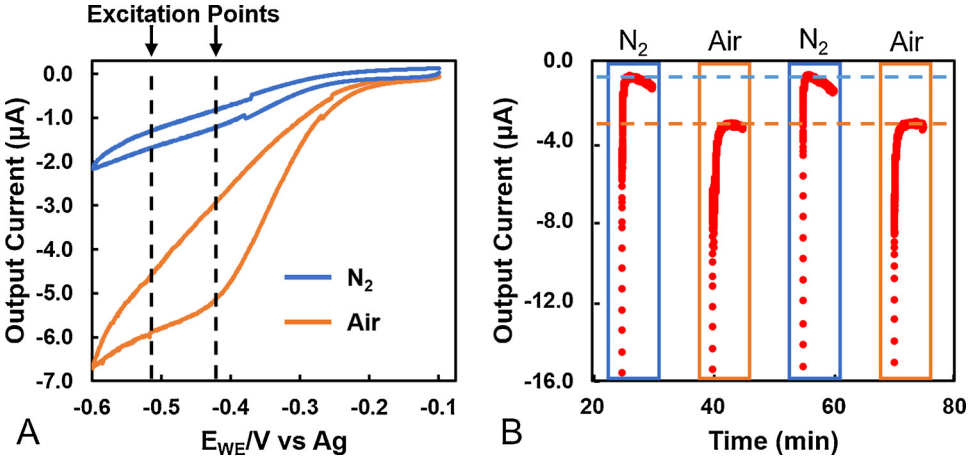

Fig. 4. Electrochemical characterization of assembled DO sensor using benchtop potentiostat. (A) Cyclic voltammogram of the sensor assembly in 0.1 M KCl solution, comparing unmodified Au sensor at an air-saturated (orange) and N_2-saturated (blue) DO state. Two excitation points were identified within the observed diffusion-limited range (plateaued current response) that correspond with the voltage bias values obtainable from the LMP91000 AFE. (B) Chronoamperogram of 0% and 100% DO saturation states using an excitation voltage of -0.42 V. Beaker is purged for four 10-minute intervals.

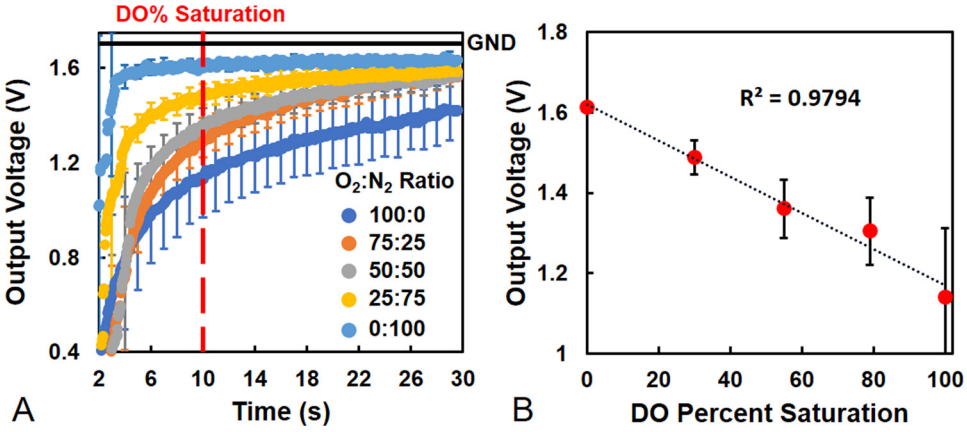

Fig. 5. Electrochemical characterization of the bPod for wireless amperometric measurements in DI water. (A) Chronoamperogram depicting the averaged output voltage recorded by the bPod with 3 repeats at a 5-minute interval (N = 3). The O_2:N_2 gas ratio was adjusted from 100:0 to 0:100 at a 25% interval. (B) Resulting calibration curve taken at 10 s and compared to the commercial polarographic DO probe.

3. Results and Discussion

3.1. Electrochemical characterization

The electrochemical response of the fabricated DO sensor was evaluated in 0.1 M KCl using the beaker-level setup. Fig. 4A presents the cyclic voltammogram of the unmodified Au sensor at both air and N_2 saturated states. Cathodic current was maximal in the potential range of -0.4 V – -0.6 V, where it shows diffusion-limited behavior (plateaued current response). As a result, two voltages, or excitation points, (vs. Ag) were identified as suitable for amperometric measurements: -0.42 V and -0.5 V. These values corresponded to the voltage biases that could be generated within the observed diffusion-limited range (plateaued current response) using the AFE, namely the LMP91000. Chronoamperometry was applied at a fixed voltage bias of -0.42 V for 45 seconds to identify a minimum dynamic range for the sensor. Fig. 4B shows the chronoamperogram alternating between a 0 and 100% DO saturation states at 10-minute intervals. By analyzing the chronoamperometric response of the sensor using the benchtop potentiostat, an average current difference of 2.5 µA was observed between the air purged state (-3.1 µA) and the N_2 sparged state (-0.6 µA). Further, during each measurement at N_2 saturation a slight drift, or decrease in the current response was seen, corresponding to an increasing DO saturation. This phenomenon was likely due to the absence of N_2 sparging into the beaker, as the solution returned to an equilibrium DO concentration (ambient air). This behavior was not observed with the FEP membrane equipped sensor or in the controlled environment of the 10-L bioreactor. However, it was found that the -0.5 V excitation voltage was more compatible with the observed output voltage bounds of the LMP91000, as determined by testing in the 2 L glass vessel. Therefore, -0.5 V was utilized as the voltage bias pulse for the bPod. This experiment verifies the viability of the electrochemical DO sensor materials and assembly for sensing at DO concentrations relevant for bioprocess monitoring applications and creates a reference system that can be used to configure the AFE (LMP91000).

Ion impermeability of the FEP membrane and the efficacy of the tape-based sensor interface were evaluated using cyclic voltammetry as described in section 2.3.1. The assembled electrochemical DO sensor was able to successfully detect DO in DI water under ambient sparged conditions, compared to the unmodified Au sensor, which was unable to measure DO in the absence of an electrolyte (KCl), as shown in Supplemental Fig. 3. The current responses were found to be -4 µA and-0.2 µA, respectively. Measurements were performed simultaneously with system sparging into the glass beaker, and no artifacts from bubble formation and agitation were observed. In this simulated environment we were unable to fully assess the effects of fouling of the sensor membrane due to accumulation of proteins and lipids, which usually lead to a deteriorated sensor response, and is the subject of ongoing research efforts. However, the sensor limitations were identified, first, within an ideal aqueous media for several hours of continuous DO monitoring. Furthermore, brief measurement of the bPod in Dulbecco Modified Eagle Medium (DMEM) with CV using the benchtop potentiostat showed no deviation from the results depicted in Supplemental Fig. 3. As a result, the bPod was found capable of monitoring DO under continuous agitation and aeration conditions, which are prevalent within the bioreactor environments.

3.2. Calibration of tethered bPod in 10-L bioreactor

The bPod was tethered to the 3.3 V power supply and submerged into the 10-L bioreactor filled with DI water for calibration at multiple DO saturation percentages, as described in section 2.3.2. The DO% saturation state measurement profile starts with a two-point calibration of 0% and 100% DO, then descends from 100% to 0% at a 25% interval (100:0. 75:25. 50:50, 25:75, and 0:100). The bPod 'CALIBRATE' state was set to excite the DO sensor at -0.5 V for 30 s. The current response was sampled every 50 ms with the BLE microcontroller with a 5-minute interval, then wirelessly transmitted to the phone app. The resulting chronoamperogram are recorded in Fig. 5A and calibrated with the inline DO probe. During the first 6 s the voltage response of the chronoamperogram increased rapidly until, after 10 s, the voltage began to saturate, allowing the different DO saturation states to become distinguishable. It was critical for the long-term operation of the bPod that the measurement duration was minimized in order to reduce the power consumption. Therefore, the DO% saturation was calculated from Supplemental Eq. (2) using the saturated voltage output observed at 10 seconds. The resulting calibration plot is shown in Fig. 5B, exhibiting a linear response (correlation coefficient $R^2 = 0.98$) with a sensitivity of 37.5 nA/DO% and limit of detection of 8.26 DO%. Based on the extracted DO% saturation at 10 s, the sensitivity was calculated using the slope of the calibration curve, and the limit of detection was derived by multiplying the standard deviation (at 10 s) by three and dividing by the sensitivity. These parameters were used to assess the bPod's sensing capabilities and the validity of the identified 10 s timepoint. Additional testing is necessary to achieve dynamic sampling at various locations for untethered experiments, which would require extrapolation of the current response at lower measurement times (i.e. 5 seconds) and correlating it to the DO% saturation.

3.3. Real-time monitoring of DO with untethered bPod in 10-L bioreactor

To evaluate the stability and continuous monitoring capabilities of the untethered system, the bPod was deployed in a 10-L glass bioreactor, controlled by the BioFlo 310 fermenter (see section 2.3.3). The bPod could freely move in the bioreactor vessel; however, the mass of the bPod modified to maintain a floating condition with the sensor fully submerged in the vessel, minimizing collisions with the bioreactor impellers and glass wall. The MEASUREMENT command, as described

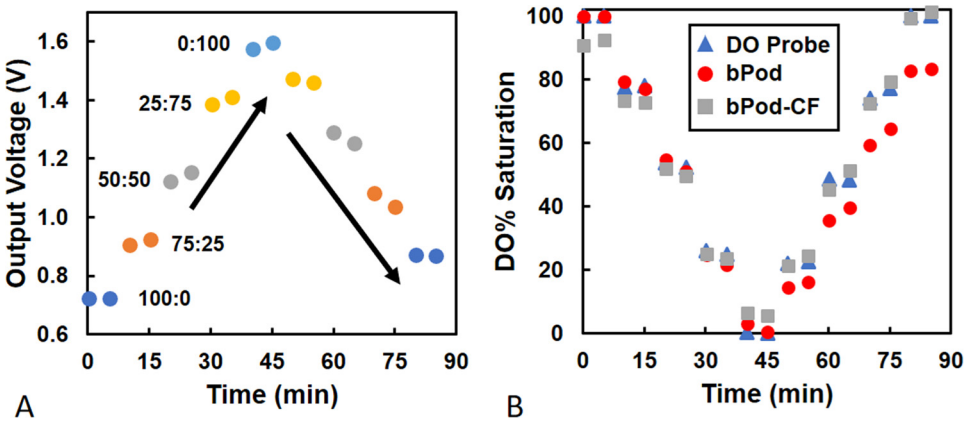

Fig. 6. Electrochemical response of untethered bPod (w/ battery) in the 10-L bioreactor setup. Gas input is alternated every 10 minutes (O_2:N_2 - 100:0, 75:25 50:50, 25:75, 0:100) over a 1.5 - h period and DO is measured at a 5-minute interval. (A) Output voltage from the bPod recorded at 10 s. (B) Comparison of the DO% saturation of the inline DO probe (blue, triangle), bPod (red, circle), and corrected bPod (bPod-CF) (gray, square).

in section 2.2.4, was utilized to perform chronoamperometric measurements of DO every 5 minutes for 1.5 hours. The DO% saturation was adjusted from 100 to 0% DO at 25% intervals every 10 minutes. Fig. 6A depicts the output voltage response of the bPod, taken at 10 seconds. In agreement with calibration results, the output voltage was found to linearly increase, inversely proportional with DO% saturation, signifying excellent reproducibility using the taped sensor interface.

It was observed that measurements taken from the DO sensor shifted slightly as the reactor dissolved oxygen was maintained at a steady level. That is, the second data point depicted at each saturation level was found to increase or decrease in the same direction as the reactor vessel. This may have been due to (1) the reactor dissolved oxygen level or (2) the electrode equilibration time. We subsequently converted these values into a DO% saturation and compared our results to the gold standard in-line polarographic DO probe, shown in Fig. 6B. The results from the polarographic probe also shifted in the same direction as the level of saturation, but to a far lesser extent. This suggests that the response time of the polarographic probe was quicker than our bPod. In Fig. 6B, we corrected the bPod values for the observed sustained shift over time using a linear correction factor to obtain the data points shown in gray boxes. The remaining discrepancy while less than 4% was likely due to error associated with differences in the response time of the probe and bPod.

Initial measurements varied less than 4% for the first 45 minutes, however, the difference between the bPod and the DO probe was observed to shift over the remaining measurements. We suspect this discrepancy may have been due to a transient degradation of either the gold or silver (reference) electrodes owing to repeated excitation. The sensor design was vastly improved over the initial attempts, which incorporated a 3D-printed electrolyte well, a PTFE membrane, and an O-ring used to bond the membrane to a snap-on 3D-printed housing. Several iterations were developed until we settled on the current tape-based sensor interface. Potential improvements are still envisioned, however we can improve the response by: increasing the ratio between the surface area of the counter and working electrodes (CE:WE > 2:1) to minimize the potential difference between CE and WE during measurements [42], or by operating at a lower voltage bias (-0.42 V). Using the data from Fig. 6A, we applied a linear calibration correction term to enable better tracking of the measurement to the Ingold polarographic electrode. For example, a suggested method to account for the shift in DO% saturation, is to apply a correction factor (CF). As shown in Supplemental Fig. 4, the absolute value of the difference between the bPod and DO probe DO% were recorded for each measurement, showing a linear deviation for values greater than 5% after 45 minutes. A linear fit was applied and reflected in Fig. 6B, where the modified bPod values with the CF (bPod-CF) show significantly reduced DO% deviation (< 4%) across later measurements (after 45 minutes), as compared to the reference inline probe. Therefore, offline correction of linear DO% saturation shifts provides a viable solution to account for degradation in the sensor response, prolonging device operation and stabilizing the DO% saturation measurement of the bPod.

The voltage regulator maintained a stable 3.3 V supply voltage from the 3.7 V Li-Po battery without degradation throughout the measurement duration. Sampling time can be extended by using a larger capacity battery, such as a CR2032 coin cell (198 mW/hr, Energizer), in order achieve operational lifetimes suitable for mammalian cell cultures [43]. While the introduced bPod platform sufficiently validates the practicality of free-floating wireless capsules for DO monitoring within bioreactors, there are additional opportunities to extend this study in terms of device scalability, sensor network size, process parameter localization, and continuous monitoring of cell culture products of interest (i.e. monoclonal antibodies). The paradigm of integrating microsystems and biosensor technologies is well positioned to not only enhance bioprocess monitoring capabilities but revolutionize the next generation of bioreactor probes for investigating product heterogeneity within bioreactors.

4. Conclusions

Growing global demand for culture products has led to the increased use of large-scale bioreactors and a shift towards parallel processing. This has increased the need for effective tools that continuously monitor cell culture parameter levels and distribution throughout the bioreactor. The presented work describes an integrated wireless platform for real-time monitoring of DO. The bPod utilizes a Clark-type DO sensor coupled with a BLE chipset for wireless data acquisition. The system was characterized with chronoamperometry in various aqueous solutions and vessels, resulting in a linear electrochemical response to changes in DO concentrations. Future efforts will focus on the miniaturization of system components to achieve a smaller form factor, assessing biocompatibility with cell media, generation and implementation of multiple sensors in parallel, and localization of individual device nodes, which may be implemented into a sensor network to distinguish the distribution of culture parameters within large-scale and single-use bioreactors. This platform presents significant progress towards scalable *in situ* applications ultimately targeting bioreactor heterogeneity. Specifically, this technology can be paired with a variety of electrochemical sensors and allow for a modular means of monitoring not only DO, but additional culture parameters. In summary, this work demonstrates a systems integration approach to achieving a wireless amperometric DO sensor for bioprocess monitoring. Integration into bioreactors and further development of similar innovative autonomous approaches enables higher control toward modulating bioreactor conditions, which will promote large scale production of increasingly complex biologics.

CRediT authorship contribution statement

Justin M. Stine: Investigation, Writing - original draft, Software. **Luke A. Beardslee:** Supervision, Validation, Methodology. **Rajendra M. Sathyam:** Software. **William E. Bentley:** Conceptualization, Funding acquisition. **Reza Ghodssi:** Conceptualization, Supervision.

Declaration of Competing Interest

The authors declare that they have no known competing financial interests or personal relationships that could have appeared to influence the work reported in this paper.

Acknowledgements

This work was funded by the National Science Foundation - Advanced Mammalian Biomanufacturing Innovation Center, NSF – AMBIC (1841506) grant. The authors acknowledge the University of Maryland Nanocenter and its FabLab for support during fabrication processes. We thank Ben Woodard and the Biotechnology Research and Education Program (BREP) at UMD for providing guidance for operating the bioreactor.

Appendix A. Supplementary data

Supplementary material related to this article can be found, in the online version, at doi:https://doi.org/10.1016/j.snb.2020.128381.

References

[1] G.P. Adams, L.M. Weiner, Monoclonal antibody therapy of cancer, Nat. Biotechnol. 23 (2005) 1147, https://doi.org/10.1038/nbt1137.
[2] G.J. Weiner, Building better monoclonal antibody-based therapeutics, Nat. Publ. Gr. 15 (2015) 361–370, https://doi.org/10.1038/nrc3930.
[3] N. Carreau, A. Pavlick, Revolutionizing treatment of advanced melanoma with immunotherapy, Surg. Oncol. (2019), https://doi.org/10.1016/j.suronc.2019.01.002.
[4] F.M. Wurm, Production of recombinant protein therapeutics in cultivated mammalian cells, Nat. Biotechnol. 22 (2004) 1393–1398, https://doi.org/10.1038/nbt1026.
[5] P. O'Mara, A. Farrell, J. Bones, K. Twomey, Staying alive! Sensors used for monitoring cell health in bioreactors, Talanta 176 (2018) 130–139, https://doi.org/10.1016/j.talanta.2017.07.088.
[6] Y. Obeidat, T. Chen, Characterization of an O2 sensor using microelectrodes, 2016 IEEE SENSORS (2016) 1–3, https://doi.org/10.1109/ICSENS.2016.7808460.
[7] A.R. Lara, E. Galindo, O.T. Ramírez, L.A. Palomares, Living with heterogeneities in bioreactors, Mol. Biotechnol. 34 (2006) 355–381, https://doi.org/10.1385/MB:34:3:355.
[8] R. Kunert, D. Reinhart, Advances in recombinant antibody manufacturing, Appl. Microbiol. Biotechnol. 100 (2016) 3451–3461, https://doi.org/10.1007/s00253-016-7388-9.
[9] Y. Zhou, L.R. Han, H.W. He, B. Sang, D.L. Yu, J.T. Feng, X. Zhang, Effects of agitation, aeration and temperature on production of a novel glycoprotein gp-1 by streptomyces kanasenisi zx01 and scale-up based on volumetric oxygen transfer coefficient, Molecules 23 (2018) 1–14, https://doi.org/10.3390/molecules23010125.
[10] L.A. Khawli, S. Goswami, R. Hutchinson, Z.W. Kwong, J. Yang, X. Wang, Z. Yao, A. Sreedhara, T. Cano, D. Tesar, I. Nijem, D.E. Allison, P.Y. Wong, Y.-H. Kao, C. Quan, A. Joshi, R.J. Harris, P. Motchnik, Charge variants in IgG1: Isolation, characterization, in vitro binding properties and pharmacokinetics in rats, MAbs 2 (2010) 613–624, https://doi.org/10.4161/mabs.2.6.13333.
[11] M. Vázquez-Rey, D.A. Lang, Aggregates in monoclonal antibody manufacturing processes, Biotechnol. Bioeng. 108 (2011) 1494–1508, https://doi.org/10.1002/bit.23155.
[12] F. Torkashvand, B. Vaziri, Main Quality Attributes of Monoclonal Antibodies and Effect of Cell Culture Components, Iran. Biomed. J. 21 (2017) 131–141, https://doi.org/10.18869/acadpub.ibj.21.3.131.
[13] S. Suresh, V.C. Srivastava, I.M. Mishra, Techniques for oxygen transfer measurement in bioreactors: a review, (2009), pp. 1091–1103, https://doi.org/10.1002/jctb.2154.
[14] O.S. Wolfbeis, Luminescent sensing and imaging of oxygen: fierce competition to the Clark electrode, Bioessays 37 (2015) 921–928, https://doi.org/10.1002/bies.201500002.
[15] J. Park, J.H. Chang, M. Choi, J.J. Pak, D.Y. Lee, Y.K. Pak, Microfabirated clark-type sensor for measuing dissolved oxygen, Proc. IEEE Sensors (2007) 1412–1415, https://doi.org/10.1109/ICSENS.2007.4388677.
[16] T.-J. Kim, T.-H. Jurng, U.-H. Chung, S.-I. Hong, Simultaneous determination of oxygen transport characteristics of six membranes by hexagonal dissolved oxygen sensor system, Sensors Actuators B Chem. 72 (2001) 11–20, https://doi.org/10.1016/S0925-4005(00)00628-6.
[17] Y. Zhang, I. Angelidaki, A simple and rapid method for monitoring dissolved oxygen in water with a submersible microbial fuel cell (SBMFC), Biosens. Bioelectron. 38 (2012) 189–194, https://doi.org/10.1016/j.bios.2012.05.032.
[18] K. Twomey, L.C. Nagle, A. Said, F. Barry, V.I. Ogurtsov, Characterisation of Nanoporous Gold for Use in a Dissolved Oxygen Sensing Application, Bionanoscience 5 (2015) 55–63, https://doi.org/10.1007/s12668-014-0161-6.
[19] F. Li, N. Vijayasankaran, A.Y. Shen, R. Kiss, A. Amanullah, Cell culture processes for monoclonal antibody production, MAbs 2 (2010) 466–479, https://doi.org/10.4161/mabs.2.5.12720.
[20] R.J. Fleischaker, A.J. Sinskey, Oxygen demand and supply in cell culture, Eur. J. Appl. Microbiol. Biotechnol. 12 (1981) 193–197, https://doi.org/10.1007/BF00499486.
[21] B. Tang, B. Qiu, S. Huang, K. Yang, L. Bin, F. Fu, H. Yang, Bioresource Technology Distribution and mass transfer of dissolved oxygen in a multi-habitat membrane bioreactor, Bioresour. Technol. 182 (2015) 323–328, https://doi.org/10.1016/j.biortech.2015.02.028.
[22] P. Gronemeyer, R. Ditz, J. Strube, Trends in Upstream and Downstream Process Development for Antibody Manufacturing, Bioeng. 1 (2014), https://doi.org/10.3390/bioengineering1040188.
[23] R.A. Potyrailo, C. Surman, W.G. Morris, T. Wortley, M. Vincent, R. Diana, V. Pizzi, J. Carter, G. Gach, Lab-scale long-term operation of passive multivariable RFID temperature sensors integrated into single-use bioprocess components, 2011 IEEE Int. Conf. RFID-Technologies Appl. (2011) 16–19, https://doi.org/10.1109/RFID-TA.2011.6068609.
[24] C. Surman, R.A. Potyrailo, W.G. Morris, T. Wortley, M. Vincent, R. Diana, V. Pizzi, J. Carter, G. Gach, Temperature-independent passive RFID pressure sensors for single-use bioprocess components, 2011 IEEE Int. Conf. RFID, RFID 2011 (2011) 78–84, https://doi.org/10.1109/RFID.2011.5764640.
[25] R.A. Potyrailo, C. Surman, A Passive Radio-Frequency Identification (RFID) Gas Sensor With Self-Correction Against Fluctuations of Ambient Temperature, Sens. Actuators. B. Chem. 185 (2013) 587–593, https://doi.org/10.1016/j.snb.2013.04.107.
[26] N. Todtenberg, T. Basmer, J. Klatt, K. Schmalz, Estimation of 433 MHz path loss in algae culture for biosensor capsule application, 2013 Eur. Microw. Conf. (2013) 712–715, https://doi.org/10.23919/EuMC.2013.6686755.
[27] N. Todtenberg, S.T. Schmitz-Hertzberg, K. Schmalz, J. Klatt, F. Jorde, B. Jüttner, R. Kraemer, Autonomous sensor capsule for usage in bioreactors, IEEE Sens. J. 15 (2015) 4093–4102, https://doi.org/10.1109/JSEN.2015.2412652.
[28] R. Zimmermann, L. Fiabane, Y. Gasteuil, R. Volk, J.F. Pinton, Characterizing flows with an instrumented particle measuring Lagrangian accelerations, New J. Phys. 15 (2013), https://doi.org/10.1088/1367-2630/15/1/015018.
[29] R. Zimmermann, L. Fiabane, Y. Gasteuil, R. Volk, J.F. Pinton, Measuring Lagrangian accelerations using an instrumented particle, Phys. Scr. 88 (2013) 1–8, https://doi.org/10.1088/0031-8949/2013/T155/014063.
[30] SmartINST, In Situ Wireless Measurements, (2015) http://webma9021.wixsite.com/smartinstnew/smartcaps-in-situ-wireless-measurem.
[31] C.M. Caffrey, K. Twomey, V.I. Ogurtsov, Development of a wireless swallowable capsule with potentiostatic electrochemical sensor for gastrointestinal track investigation, Sensors Actuators B Chem. 218 (2015) 8–15, https://doi.org/10.1016/J.SNB.2015.04.063.
[32] Abbot Laboratories, FreeStyle Libre, (2018) https://www.freestylelibre.us/.
[33] J. Kim, S. Imani, W.R. de Araujo, J. Warchall, G. Valdés-Ramírez, T.R.L.C. Paixão, P.P. Mercier, J. Wang, Wearable salivary uric acid mouthguard biosensor with integrated wireless electronics, Biosens. Bioelectron. 74 (2015) 1061–1068, https://doi.org/10.1016/j.bios.2015.07.039.
[34] H. Yoon, X. Xuan, S. Jeong, J.Y. Park, Wearable, robust, non-enzymatic continuous glucose monitoring system and its in vivo investigation, Biosens. Bioelectron. 117 (2018) 267–275, https://doi.org/10.1016/j.bios.2018.06.008.
[35] A. Pal, D. Goswami, H.E. Cuellar, B. Castro, S. Kuang, Biosensors and Bioelectronics Early detection and monitoring of chronic wounds using low-cost, omniphobic paper-based smart bandages, Biosens. Bioelectron. 117 (2018) 696–705, https://doi.org/10.1016/j.bios.2018.06.060.
[36] R.C. Huiszoon, S. Subramanian, P.R. Rajasekaran, L.A. Beardslee, W.E. Bentley, R. Ghodssi, Flexible Platform for In Situ Impedimetric Detection and Bioelectric Effect Treatment of Escherichia coli Biofilms, IEEE transactions on bio-medical engineering 9294 (2018) 1–9, https://doi.org/10.1109/TBME.2018.2872896.
[37] G.E. Banis, S. Member, L.A. Beardslee, J.M. Stine, R.M. Sathyam, R. Ghodssi, Gastrointestinal Targeted Sampling and Sensing via Embedded Packaging of Integrated Capsule System, J. Microelectromechanical Syst. (2019) 1–7, https://doi.org/10.1109/JMEMS.2019.2897246 PP.
[38] Y.L. Kong, X. Zou, C.A. McCandler, A.R. Kirtane, S. Ning, J. Zhou, A. Abid, M. Jafari, J. Rogner, D. Minahan, J.E. Collins, S. McDonnell, C. Cleveland, T. Bensel, S. Tamang, G. Arrick, A. Gimbel, T. Hua, U. Ghosh, V. Soares, N. Wang, A. Wahane, A. Hayward, S. Zhang, B.R. Smith, R. Langer, G. Traverso, 3D-Printed Gastric Resident Electronics, Adv. Mater. Technol. 1800490 (2018) 1800490, https://doi.org/10.1002/admt.201800490.
[39] L.C. Clark, Monitor and Control of Blood and Tissue Oxygen, Trans. Am. Soc. Artif. Intern. Organs. 2 (1956) 41–48.
[40] J. Gębicki, A. Kloskowski, W. Chrzanowski, P. Stepnowski, J. Namiesnik, Application of Ionic Liquids in Amperometric Gas Sensors, Crit. Rev. Anal. Chem. 46 (2016) 122–138, https://doi.org/10.1080/10408347.2014.989957.
[41] B. Isailovic, B. Rees, M. Kradolfer, Fluid dynamics of a single-use, stirred-tank

bioreactor for mammalian cell culture, Bioprocess Int. 13 (2015).
[42] M. Tian, C. Cousins, D. Beauchemin, Y. Furuya, A. Ohma, G. Jerkiewicz, Influence of the Working and Counter Electrode Surface Area Ratios on the Dissolution of Platinum under Electrochemical Conditions, ACS Catal. 6 (2016) 5108–5116, https://doi.org/10.1021/acscatal.6b00200.
[43] S. Xu, J. Gavin, R. Jiang, H. Chen, Bioreactor productivity and media cost comparison for different intensified cell culture processes, Biotechnol. Prog. 33 (2017) 867–878, https://doi.org/10.1002/btpr.2415.

Justin Stine is pursuing his PhD in Electrical Engineering at the University of Maryland, College Park. His research interests include the development of embedded systems, specifically design and integration of readout circuits with fabricated micro/nanoscale sensors toward environmental monitoring

Luke Beardslee is a visiting scholar at the Institute for Systems Research at the University of Maryland, College Park. He holds a PhD in electrical engineering from the Georgia Institute of Technology and he is also a physician; his research interests include micro/nanoscale fabrication, MEMS sensors, and embedded systems for implantable, ingestible, and environmental sensing applications.

Rajendra Sathyam received his ME in Robotics at the University of Maryland, College Park, and is currently a Machine Learning software engineer at Panasonic automotive systems of America. His research interests are computer vision, machine learning, and robotics.

William Bentley is a professor in the Fischell Department of Bioengineering at the University of Maryland, College Park. He is the Robert E. Fischell Distinguished Chair of Engineering and the Inaugural Director of the Robert E. Fischell Institute for Biomedical Devices. His research interests are in biomolecular & metabolic engineering, cell-cell communication, heterologous protein expression, and device/bio interfaces.

Reza Ghodssi is a professor in the Department of Electrical and Computer Engineering at the University of Maryland, College Park. He is the Herbert Rabin Distinguished Chair of engineering. His research interests are in the design and development of micro/nano/bio devices and systems for chemical and biological sensing, small-scale energy conversion, and harvesting with a strong emphasis toward healthcare applications.